SUPPLEMENTAL MATERIAL

Mitochondria-encoded circRNA mecciRNR2 promotes hepatocellular carcinoma progression by stabilizing HNRNPA1 and suppressing IGFBP3 expression

Juzheng Sui[1,4], Jingxin Li[1,4], Kang Xie[2,4], Liang Shi[3], Ge Shan[1*], Xu Liu[1*]

[1] *Department of Obstetrics and Gynecology, The First Affiliated Hospital of USTC, The RNA Institute, School of Basic Medical Sciences, Center for Advanced Interdisciplinary Science and Biomedicine of IHM, Division of Life Science and Medicine, University of Science and Technology of China, Hefei 230027, China.*

[2] *Department of Neurosurgery, Affiliated Lianyungang Hospital of Xuzhou Medical University, Lianyungang, Jiangsu, 222000, China.*

[3] *Department of General Surgery, Sir Run Run Shaw Hospital, School of Medicine, Zhejiang University, Hangzhou, 310016, China.*

[4]*Authors contributed equally to this work.*

[*] *Corresponding author: shange@ustc.edu.cn (Ge Shan), liuxu00@ustc.edu.cn (Xu Liu).*

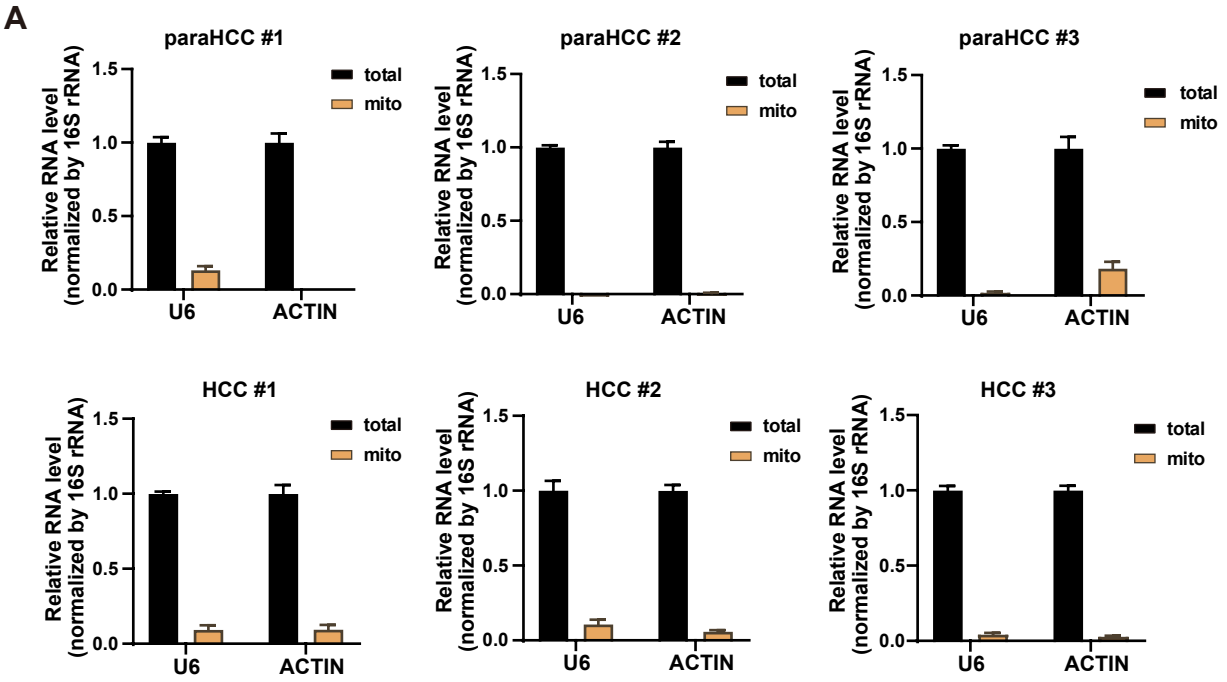
This PDF file includes:

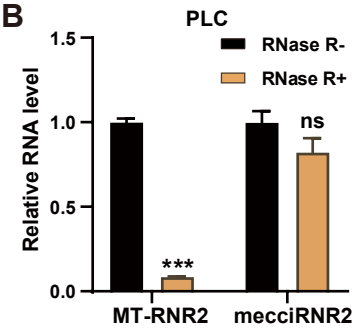
Figures S1–S7

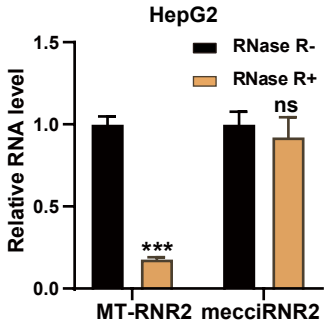
Legends for Figures S1–S7

Legends for Supplementary Tables

Figure S1



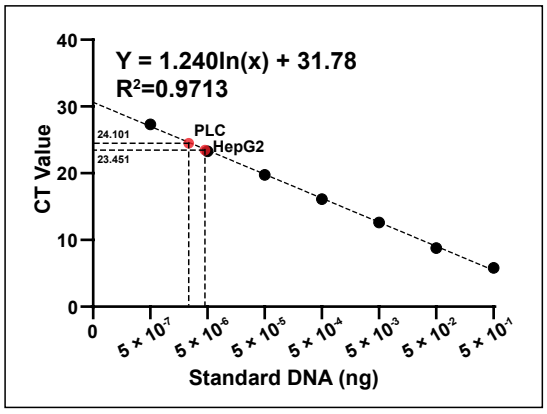


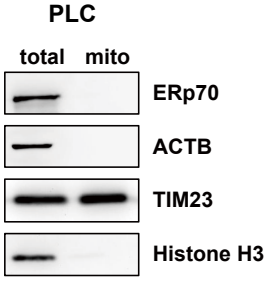


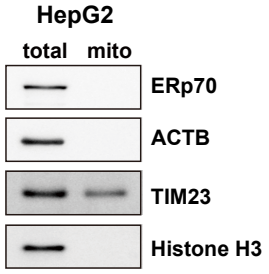
D

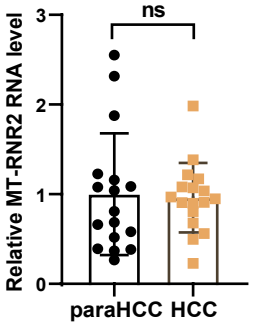
mecciRNR2 copy number per cell

HepG2	PLC
~156	~101









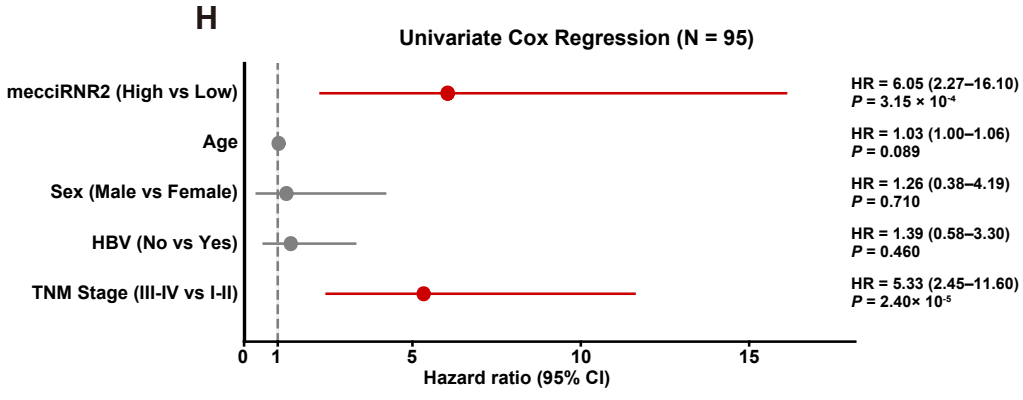


Figure S2

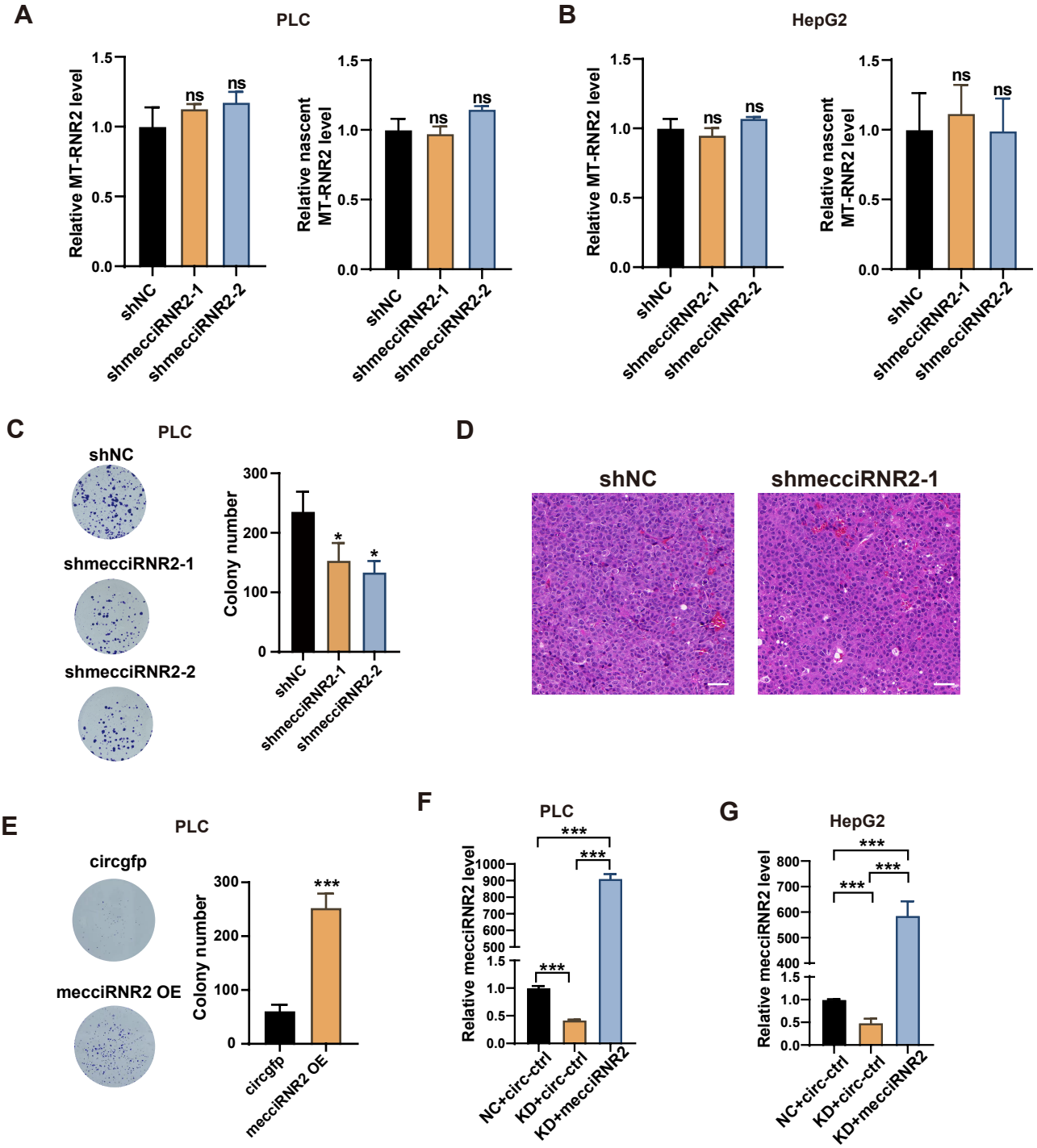

A
PLC
Relative MT-RNR2 level
Relative nascent MT-RNR2 level
ns
shNC
shmecciRNR2-1
shmecciRNR2-2
B
HepG2
C
PLC
shNC
shmecciRNR2-1
shmecciRNR2-2
Colony number
D
shNC
shmecciRNR2-1
E
PLC
circgfp
mecciRNR2 OE
F
PLC
Relative mecciRNR2 level
NC+circ-ctrl
KD+circ-ctrl
KD+mecciRNR2
G
HepG2

Figure S3

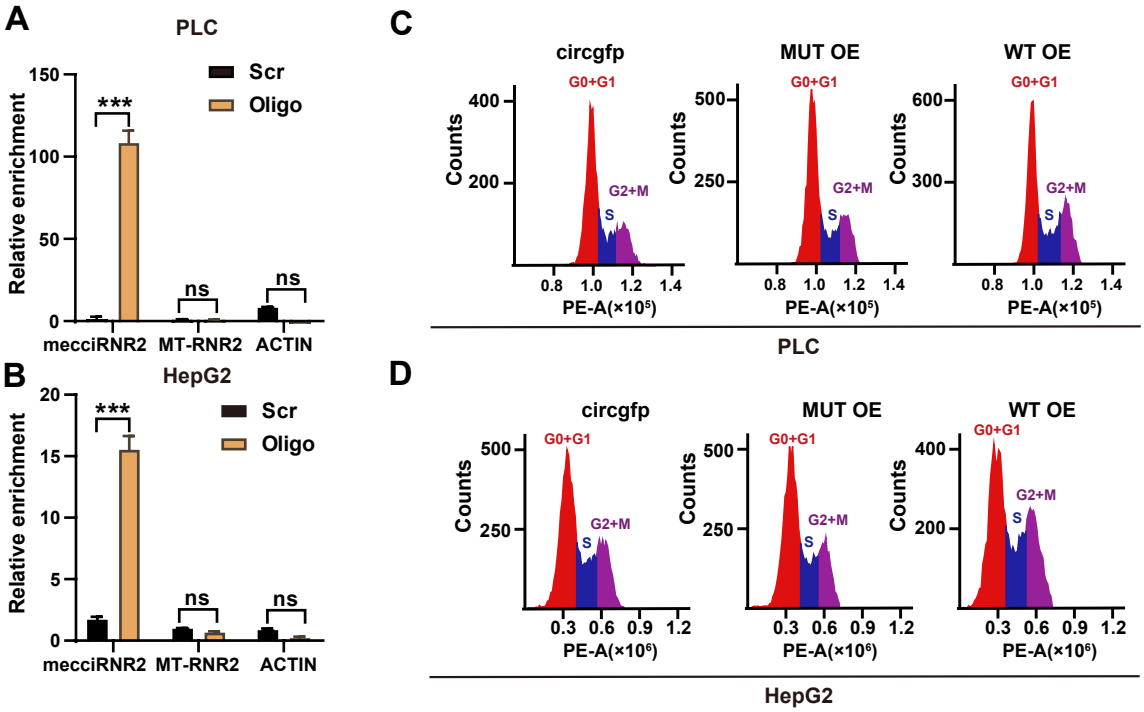

A
PLC
Scr
Oligo
Relative enrichment
150
100
50
0
***
ns
ns
mecciRNR2
MT-RNR2
ACTIN
B
HepG2
Scr
Oligo
Relative enrichment
20
15
10
5
0
***
ns
ns
mecciRNR2
MT-RNR2
ACTIN
C
circgfp
MUT OE
WT OE
Counts
G0+G1
G2+M
S
PE-A(×10⁵)
PLC
D
circgfp
MUT OE
WT OE
Counts
G0+G1
G2+M
S
PE-A(×10⁶)
HepG2

Figure S4

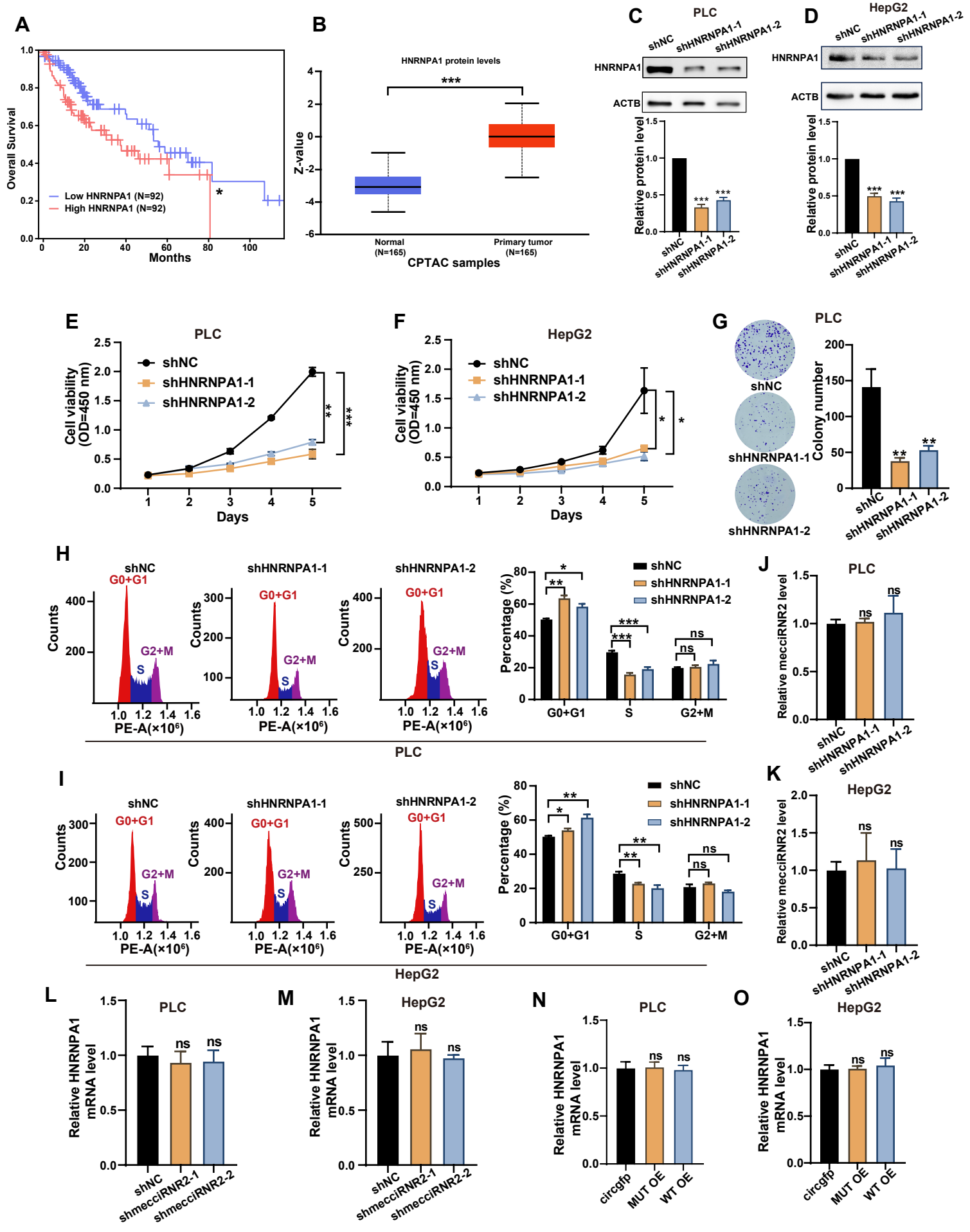

A
Overall Survival
Months
Low HNRNPA1 (N=92)
High HNRNPA1 (N=92)
B
HNRNPA1 protein levels
Z-value
Normal (N=165)
Primary tumor (N=165)
CPTAC samples
C
PLC
shNC
shHNRNPA1-1
shHNRNPA1-2
HNRNPA1
ACTB
Relative protein level
D
HepG2
E
PLC
Cell viability (OD=450 nm)
Days
F
HepG2
G
PLC
Colony number
H
shNC
shHNRNPA1-1
shHNRNPA1-2
G0+G1
S
G2+M
Counts
PE-A(×10⁶)
Percentage (%)
PLC
I
HepG2
J
PLC
Relative mecciRNR2 level
K
HepG2
L
PLC
Relative HNRNPA1 mRNA level
shmecciRNR2-1
shmecciRNR2-2
M
HepG2
N
PLC
circgfp
MUT OE
WT OE
O
HepG2

Figure S5

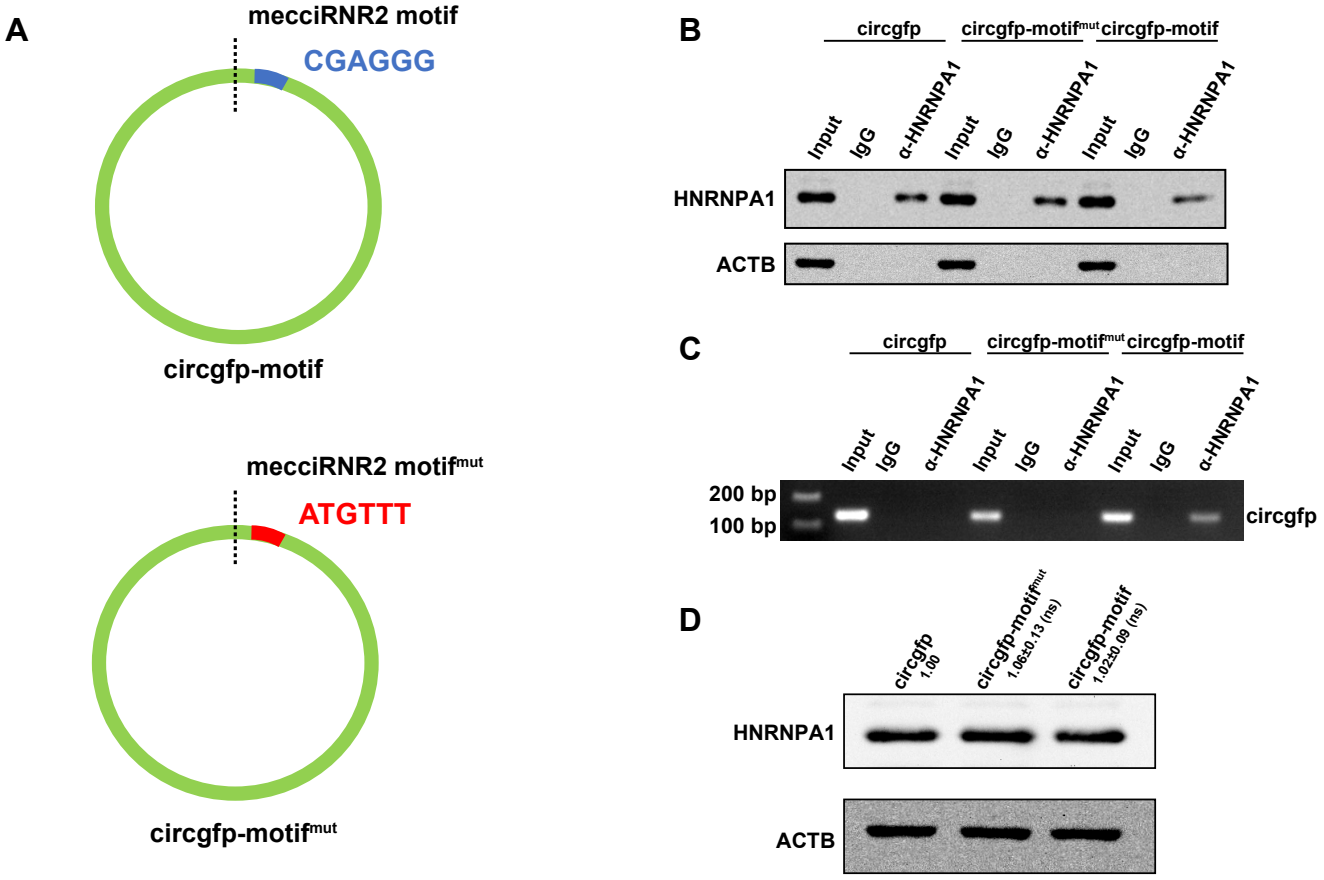

A
mecciRNR2 motif
CGAGGG
circgfp-motif
mecciRNR2 motif^mut
ATGTTT
circgfp-motif^mut
B
circgfp
circgfp-motif^mut
circgfp-motif
Input
IgG
α-HNRNPA1
HNRNPA1
ACTB
C
200 bp
100 bp
circgfp
D
circgfp
1,00
circgfp-motif^mut
1,06±0.13 (ns)
circgfp-motif
1,02±0.09 (ns)
HNRNPA1
ACTB

Figure S6

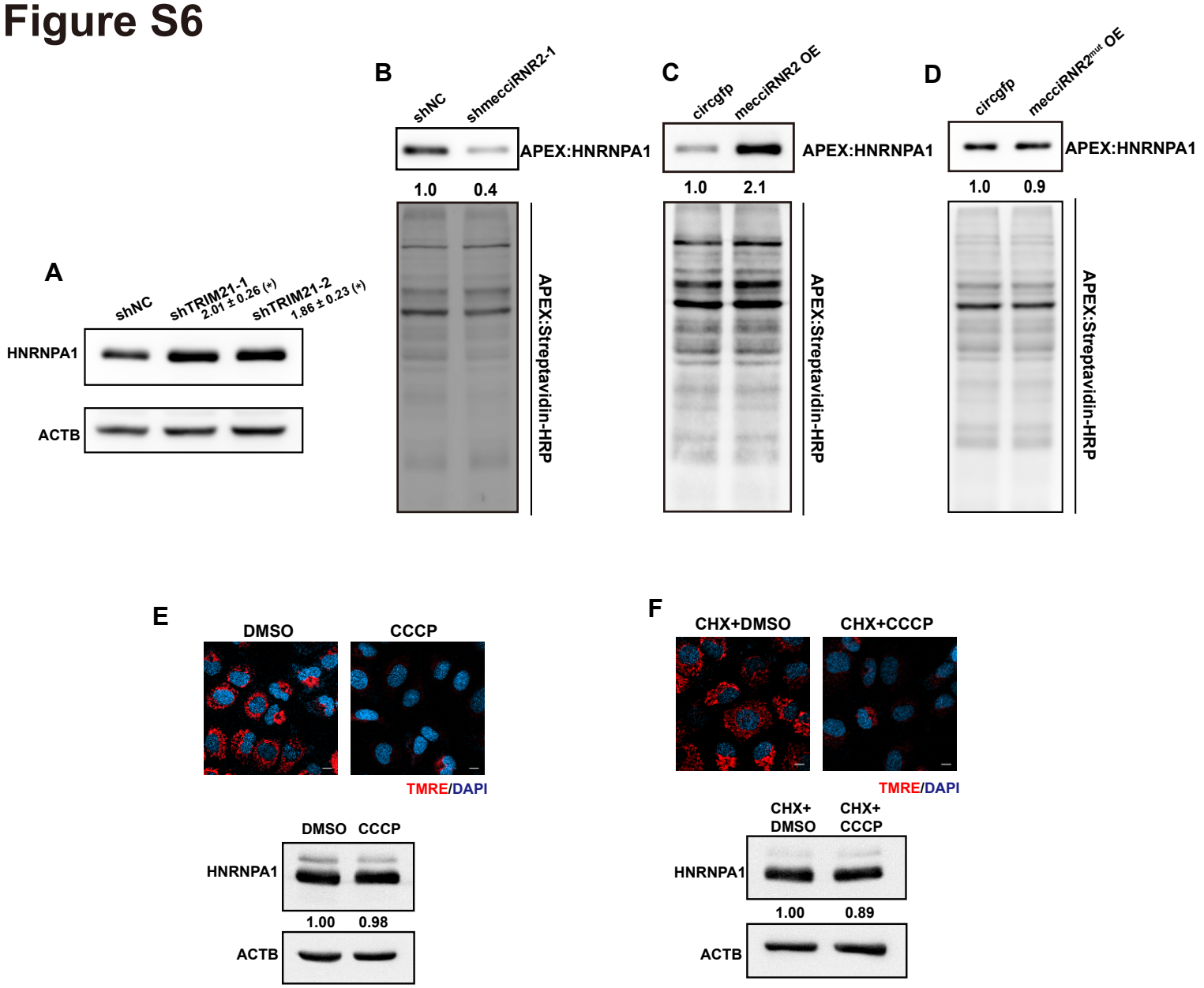

A
shNC
shTRIM21-1
2.01 ± 0.26 (*)
shTRIM21-2
1.86 ± 0.23 (*)
HNRNPA1
ACTB
B
shNC
shmecciRNR2-1
APEX:HNRNPA1
1.0
0.4
APEX:Streptavidin-HRP
C
circgfp
mecciRNR2 OE
APEX:HNRNPA1
1.0
2.1
APEX:Streptavidin-HRP
D
circgfp
mecciRNR2mut OE
APEX:HNRNPA1
1.0
0.9
APEX:Streptavidin-HRP
E
DMSO
CCCP
TMRE/DAPI
DMSO
CCCP
HNRNPA1
1.00
0.98
ACTB
F
CHX+DMSO
CHX+CCCP
TMRE/DAPI
CHX+ DMSO
CHX+ CCCP
HNRNPA1
1.00
0.89
ACTB

Figure S7

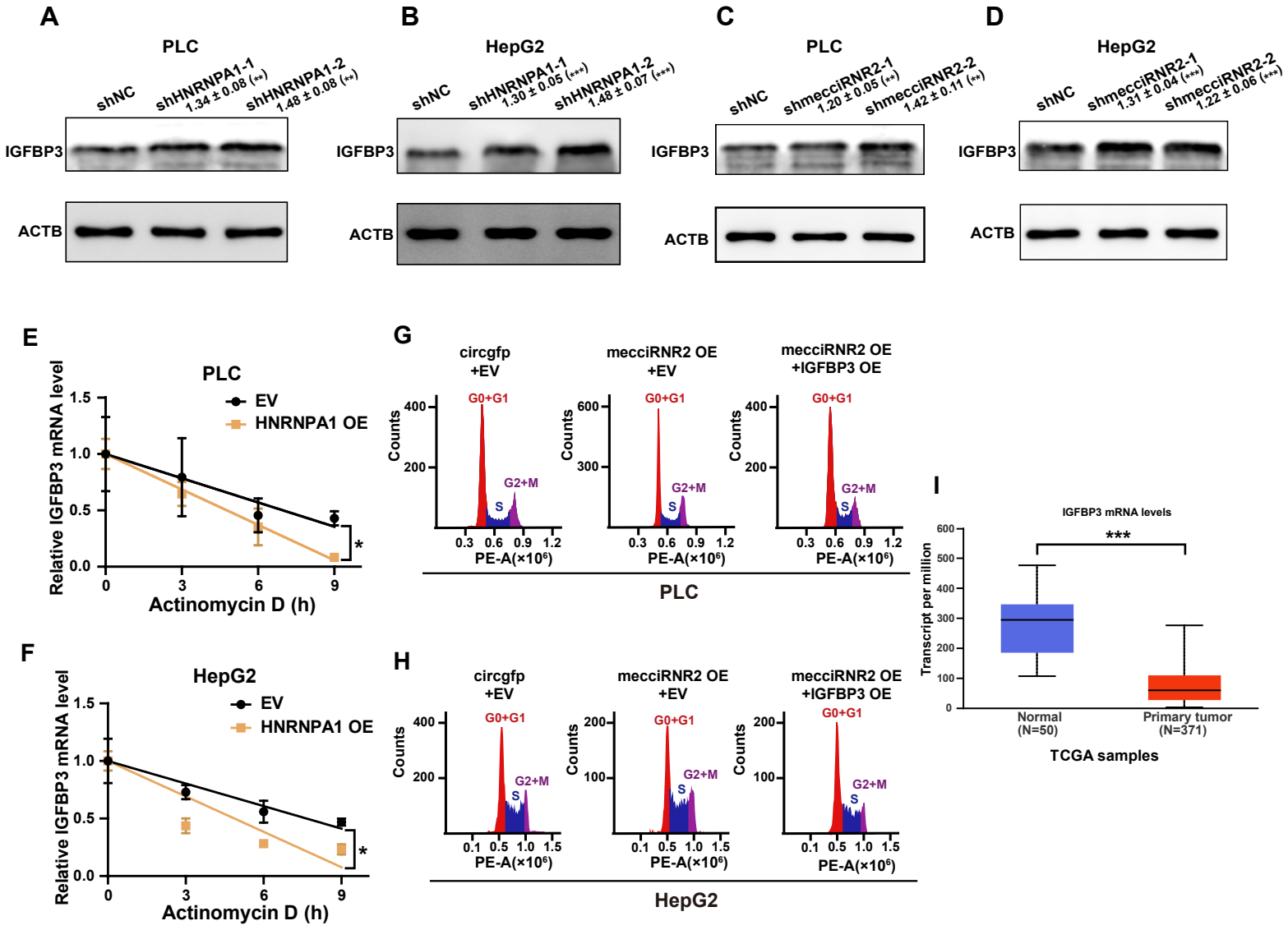

A
PLC
shNC
shHNRNPA1-1
1.34 ± 0.08 (**)
shHNRNPA1-2
1.48 ± 0.08 (**)
IGFBP3
ACTB
B
HepG2
shNC
shHNRNPA1-1
1.30 ± 0.05 (***)
shHNRNPA1-2
1.48 ± 0.07 (***)
IGFBP3
ACTB
C
PLC
shNC
shmecciRNR2-1
1.20 ± 0.05 (**)
shmecciRNR2-2
1.42 ± 0.11 (**)
IGFBP3
ACTB
D
HepG2
shNC
shmecciRNR2-1
1.31 ± 0.04 (***)
shmecciRNR2-2
1.22 ± 0.06 (***)
IGFBP3
ACTB
E
PLC
EV
HNRNPA1 OE
Relative IGFBP3 mRNA level
Actinomycin D (h)
F
HepG2
EV
HNRNPA1 OE
Relative IGFBP3 mRNA level
Actinomycin D (h)
G
circgfp +EV
mecciRNR2 OE +EV
mecciRNR2 OE +IGFBP3 OE
Counts
G0+G1
S
G2+M
PE-A(×10⁶)
PLC
H
circgfp +EV
mecciRNR2 OE +EV
mecciRNR2 OE +IGFBP3 OE
Counts
G0+G1
S
G2+M
PE-A(×10⁶)
HepG2
I
IGFBP3 mRNA levels
***
Transcript per million
Normal (N=50)
Primary tumor (N=371)
TCGA samples

Figure legends for supplementary figures

Fig. S1 Validation of mitochondrial purification, characterization of mecciRNR2, and its clinical relevance in HCC.

A RT-qPCR showing the quality of purified mitochondria from three pairs of liver cancer tissues (HCC) and adjacent non-tumor tissues (paraHCC). total, whole cell level; mito, mitochondria level; U6, nuclear marker; ACTIN, cytoplasmic marker. **B**, **C** RT-qPCR showing resistance of mecciRNR2 to RNase R digestion in PLC (**B**) and HepG2 (**C**) cells. MT-RNR2, negative control. **D**, Copy numbers of mecciRNR2 in HepG2 and PLC cells. Conventional quantitative PCR was used in the analysis. Standard curve showing the relationship between Ct values and serial dilutions of the mecciRNR2 PCR amplicon generated using divergent primers. **E**, **F** Western blotting showing the quality of purified mitochondria from PLC (**E**) and HepG2 (**F**). ERp70, endoplasmic reticulum marker; ACTB, cytoplasmic marker; TIM23, mitochondrial marker; Histone H3, nuclear marker. **G** RT-qPCR analysis of MT-RNR2 in total RNA isolated from 16 pairs of HCC and paraHCC tissues. **H** Univariate Cox proportional hazards regression analysis of overall survival in 95 patients (because TNM stage information was unavailable for five of the 100 HCC patients) with HCC. Variables included mecciRNR2 expression status, age, sex, HBV infection status, and TNM stage (III–IV vs. I–II). In **B**, **C**, data are shown as mean±SD from n=3 independent experiments. *P*-values are from two-tailed Student's *t*-tests (**B**, **C**, **G**) and the Wald test (H). ns, not significant; ***$P < 0.001$.

Fig. S2 mecciRNR2 promotes the proliferation of HCC cells.

A, **B** RT-qPCR analysis of MT-RNR2 and nascent MT-RNR2 expression in mecciRNR2 knockdown PLC (**A**) and HepG2 (**B**) cells. **C** Colony formation assays for PLC cells with mecciRNR2 knockdown. **D** H&E staining of xenografted tumors from mecciRNR2 knockdown HepG2 cells and the control cells. Scale bar, 100 μm. **E** Colony formation assays for PLC cells with mecciRNR2 overexpression. circgfp, cells transfected with a plasmid expressing a circular RNA containing the *gfp* sequence, served as a negative control. **F**, **G** RT-qPCR showing the overall cellular mecciRNR2 level in mecciRNR2 knockdown PLC (**F**) and HepG2 (**G**) cells after transfection of *in vitro* synthesized mecciRNR2. Data are shown as mean±SD from n=3 independent experiments. *P*-values are from two-tailed Student's *t*-tests. ns, not significant; *$P <$

0.05; ***$P < 0.001$.

Fig. S3 mecciRNR2 pulldown efficiency and cell cycle assay upon mecciRNR2 overexpression.

A, **B** RT-qPCR showing the RNA enrichment efficiency of mecciRNR2 pulldown in PLC (**A**) and HepG2 (**B**) cells. Scr, oligos with scrambled sequences; MT-RNR2, linear counterpart of mecciRNR2; ACTIN, negative control. **C, D** Representative cell-cycle histograms of PLC (**C**) and HepG2 (**D**) cells overexpressing wild-type (WT OE) or HNRNPA1-binding motif mutant mecciRNR2 (MUT OE). In **A**, **B**, data are shown as mean±SD from n=3 independent experiments; *P*-values are from two-tailed Student's *t*-tests.

Fig. S4 Knockdown of HNRNPA1 suppresses HCC proliferation, and knockdown or overexpression of mecciRNR2 does not alter HNRNPA1 mRNA levels.

A Kaplan-Meier analysis of overall survival according to HNRNPA1 expression in 184 HCC patients using the GEPIA3 website. **B** HNRNPA1 protein expression in HCC and normal liver tissues based on the CPTAC dataset, analyzed using the UALCAN portal. Z-values represent $\log_2$ spectral count ratio values from CPTAC, which were first normalized within each sample profile, then normalized across samples. **C**, **D** Knockdown efficiency of HNRNPA1 verified by Western blotting in PLC (**C**) and HepG2 (**D**) cells. Quantification of HNRNPA1 protein levels is shown. ACTB, loading control. **E, F** Cell proliferation measured by CCK-8 assay in HNRNPA1-knockdown PLC (**E**) and HepG2 (**F**) cells. **G** Colony formation assays for PLC cells with HNRNPA1 knockdown. **H**, **I** Cell-cycle distribution analyzed by flow cytometry in HNRNPA1-knockdown PLC (**H**) and HepG2 (**I**) cells. **J**, **K** The expression level of mecciRNR2 quantified by RT-qPCR in HNRNPA1-knockdown PLC (**J**) and HepG2 (**K**) cells. **L**, **M** The expression level of HNRNPA1 mRNA quantified by RT-qPCR in mecciRNR2-knockdown PLC (**L**) and HepG2(**M**) cells. **N**, **O** The expression level of HNRNPA1 mRNA quantified by RT-qPCR in PLC (**N**) and HepG2(**O**) cells overexpressing mecciRNR2 or mecciRNR2^{mut} (abolishing HNRNPA1 binding). Data are shown as mean±SD. In **C**, **D**, **G**–**O**, n=3 independent experiments; *P*-values are from two-tailed Student's *t*-tests. In **E**, **F**, n=6 experimental replicates for each cell line; *P*-values are from two-way ANOVA. ns, not significant; *$P < 0.05$; **$P < 0.01$; ***$P < 0.001$.

Figure S5. The HNRNPA1-binding motif alone is insufficient to modulate HNRNPA1 protein abundance.

A Schematic illustration of circgfp constructs with insertion of the wild-type or mutant HNRNPA1-binding motif derived from mecciRNR2 near the back-splice junction. **B** RIP against HNRNPA1 (α-HNRNPA1) was performed in PLC cells expressing circgfp, circgfp harboring the HNRNPA1-binding motif (circgfp motif), or circgfp harboring the mutant motif (circgfp motif^{mut}). circgfp serves as a negative control. Western blotting confirms successful IP of HNRNPA1. **C** Enrichment of circgfp RNA in HNRNPA1 RIP samples was detected by semi-quantitative RT-PCR followed by gel electrophoresis. **D** The protein levels of HNRNPA1 detected by Western blotting in PLC cells expressing circgfp, circgfp harboring the HNRNPA1-binding motif, or circgfp harboring the mutant motif. Data are shown as mean±SD from n=3 independent experiments; *P*-values are from two-tailed Student's *t*-tests; ns, not significant.

Fig. S6 Knockdown of TRIM21 increases HNRNPA1 protein levels and mitochondrial import of HNRNPA1 might not influence its protein stability.

A Western blotting detecting HNRNPA1 protein levels upon TRIM21 knockdown. Quantification of HNRNPA1 protein levels is shown. ACTB serves as a loading control. **B–D** PLC cells stably expressing mecciRNR2 shRNA (**B**), mecciRNR2 (**C**), or mecciRNR2^{mut} (**D**), together with engineered mitochondrial matrix-targeted APEX2 (matrix-APEX2), were subjected to APEX2-mediated proximity biotinylation. The APEX2-catalyzed biotinylated HNRNPA1 (APEX2: HNRNPA1) level in mitochondria was analyzed by Western blotting. The quantification of mitochondrial APEX2: HNRNPA1 (normalized to the overall biotinylated mitochondrial proteins) is shown. APEX: Streptavidin-HRP, total biotinylated mitochondrial matrix proteins. **E**, **F** Representative images of tetramethylrhodamine methyl ester (TMRE) staining in PLC cells following CCCP treatment, without (**E**) or with (**F**) co-treatment with cycloheximide (CHX). Mitochondrial membrane potential is reflected by TMRE signals. Scale bar, 10 μm. The HNRNPA1 protein level detected by Western blotting is shown. ACTB serves as a loading control.

Fig. S7 HNRNPA1 and mecciRNR2 regulate IGFBP3 expression.

A, **B** The protein levels of IGFBP3 detected by Western blotting in PLC (**A**) and HepG2 (**B**) cells under HNRNPA1 knockdown. Quantification of the IGFBP3 protein level is

shown. **C**, **D** The protein levels of IGFBP3 detected by Western blotting in PLC (**C**) and HepG2 (**D**) cells under mecciRNR2 knockdown. Quantification of the IGFBP3 protein level is shown. **E**, **F** Degradation rate of IGFBP3 mRNA following transcriptional inhibition with actinomycin D for the indicated time periods in PLC (**E**) and HepG2 (**F**) cells overexpressing HNRNPA1. **G**, **H** Representative cell-cycle histograms in mecciRNR2-overexpressing PLC (**G**) and HepG2 (**H**) cells following IGFBP3 restoration. **I** IGFBP3 mRNA expression in HCC and normal liver tissues based on the TCGA-LIHC dataset, analyzed using the UALCAN portal. In **A–F**, data are shown as mean±SD from n=3 independent experiments; *P*-values are from two-tailed Student's *t*-tests (**A**–**D**) and two-way ANOVA (**E**, **F**); **P* < 0.05; ***P* < 0.01; ****P* < 0.001.

Table S1 The basic demographics of the cohort of 100 HCC patients.

Table S2 Proteins identified from mecciRNR2 pulldown followed by mass spectrometry (MS).

Table S3 List of 69 overlap genes and their associated KEGG pathways.

Table S4 Primers and oligos used in this study.